PBG-enhanced Inductor

Hsien-Shun Wu and Ching-Kuang C. Tzuang

Institute of Electrical Communication Engineering

National Chiao Tung University, Hsinchu, TAIWAN

Abstract — **A novel inductor configuration, consisting of a two-dimensional photonic bandgap (PBG) periodical array in addition to the existing inductor, e.g., spiral inductor, is built, analyzed, and tested. Measurements show that a one-turn, 13.1 mm long spiral inductor (3 mm by 3 mm) placed on a PBG ground plane made of unit cells using coupled inductors of dimension 1.5 mm by 1.5 mm on Roger 4003™ substrates can increase the inductance by 34%, reduce the series resistance by 45%, improve the Q-factor by 33%, and extend the peak Q-factor frequency by 14% as compared to the conventional spiral inductor of the same size. Dispersion characteristics of both PBG-enhanced and conventional spiral inductors are reported.**

I. INTRODUCTION

Lumped inductor is one of the most well-known, widely used passive devices for microwave impedance matching. Rigorous analyses and designs of inductor are also well established by means of full-wave simulators in both frequency-domain and time-domain [1,2] as well as close-form formula directly related to the geometry of inductor [3,4]. Planar spiral inductor, realized by multi-layered substrates, however, is the most familiar one incorporated in RFIC, LTCC MIC, and hybrid MIC [5]. The guideline to design high-performance spiral inductor has been constantly refined through years [6].

This paper reports a new technique to improve the existing design of planar spiral inductor by incorporating a photonic bandgap (PBG) structure under the inductor as a ground plane substitute. Itoh et al. reported that the guiding characteristics of microstrip is significantly altered by the UC-PBG (Uniplanar Compact Photonic Bandgap) ground plane, resulting in the increase of slow-wave factor of the bond mode in the frequency band below the first stopband of the PBG [7]. Similar principle leads to the design of the PBG-enhanced inductor as described in Section II. Section III investigates two spiral inductors, showing theoretically and experimentally how the existing inductor designs can be improved by the new inductor configuration. Section IV concludes the paper.

II. PBG-ENHANCED INDUCTOR: DESIGN AND THEORY

The concept of PBG-enhanced inductor is illustrated in parts (a) and (b) of Fig.1, where substituting the uniform ground plane of the conventional spiral inductor (part (b)) by a PBG ground plane creates the new inductor configuration. The PBG ground plane is made of a thin, two-sided, printed-circuit board. On one side of the PBG ground plane are the coupled disconnected rectangular coils, of which the centers are connected by via through holes to the other side containing connected, rectangular coils. Similar PBG structure was reported for the EME (electric-magnetic-electric) microstrip design as a slow-wave device [8,9]. The spiral inductor has one turn and another via through hole allowing an overpass for external connection. Fig.1 shows the dimensions of the spiral inductors and PBG cells incorporated for the PBG-enhanced spiral inductor. Notice that the inductors appear in parts (a) and (b) of Fig.1 are identical except the ground planes are different.

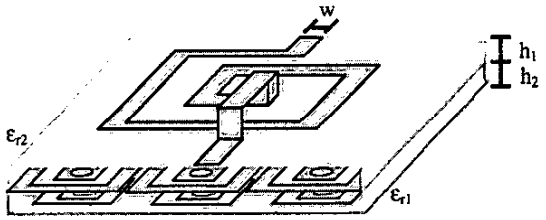

(a) PBG-enhanced inductor

0-7803-7239-5/02/$10.00 © 2002 IEEE

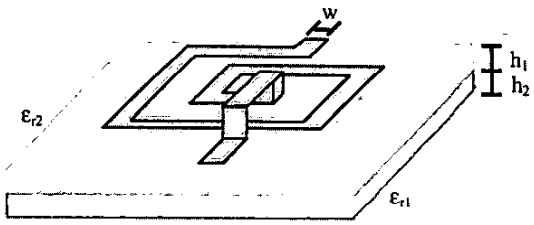

(b) Conventional inductor

Fig.1 **Generic spiral Inductor; inductor:** one turn, W=0.25 mm, gap between edges=0.25 mm, via diameter = 0.4 mm, total length = 13.1 mm, ε_{r1}= ε_{r2}= 3.38, h_1=h_2=0.2 mm, tanδ_1=tanδ_2=0.002, metal thickness= 17 um for all metal layers; **PBG periodic structure:** one-turn coupled inductors (top and bottom), W=0.2 mm, gap between edges=0.2 mm, via diameter=0.4 mm, total inductor length= 6 mm (top), 7 mm (bottom)

Rigorous field-theory analyses show that the microstrip on the PBG ground plane of Fig.1 (a) exhibits higher slow-wave factor and characteristic impedance than its conventional microstrip on uniform ground plane. This implies that the inductance per unit length of microstrip on PBG ground plane of the present design is higher than the conventional one, resulting in a higher inductance value for the PBG-enhanced inductor.

Furthermore, as shown in Fig.1 (a), the conventional spiral inductor should suffer the eddy-current losses since the uniform ground plane has finite conductivities in most practical case studies. The eddy currents of the PBG-enhanced inductor of Fig.1 (b), are disturbed by the PBG structures, where the orientation of the induced currents of the PBG ground plane often oppose to the directions of eddy currents of the conventional spiral inductor.

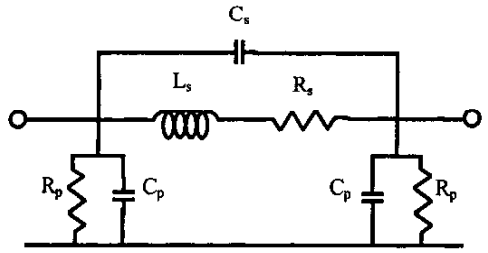

Fig.2 The equivalent circuit model of the spiral inductors of Fig.1

Fig.2 illustrates a practical circuit model of the spiral inductors shown in Fig.1 [6]. L_s, R_s, C_s, R_p and C_p correspond to the self- inductance, combined resistive and eddy-current losses, overlapping capacitance, substrate losses, substrate capacitance of the spiral inductor, respectively. Section III will show that L_s is increased and R_s is reduced simultaneously when the PBG-enhanced inductor is applied.

III. DISPERSION CHARACTERISTICS OF SPIRAL INDUCTORS: PBG-ENHANCED AGAINST CONVENTIONAL

Theoretical analyses based on full-wave integral equation simulator and experimental verification of prototype are invoked for the comparative studies of the inductor properties of the conventional and new approaches. First, we obtain theoretical and measured two-port scattering-parameters of the spiral inductors. Second, the two-port scattering-parameters are converted to the ABCD matrix representation of a transmission line equivalent circuit of the two-port spiral inductor. Since the absolute value of $\gamma\ell$ is much less than unity, where γ is the complex propagation constant of the transmission line equivalent circuit and ℓ is the length of the spiral inductor, the parallel R_p-C_p of Fig.2 can be expressed by $2Z_o$ divided by $\gamma\ell$. Z_o is the characteristic impedance of the transmission line equivalent circuit [6].

In our particular case studies, C_s is relatively small and can be neglected. The complex impedance of the series L_s-R_s can be expressed by the product of Z_o and $\gamma\ell$ [6].

Fig.3 plots the theoretical and measured L_s of the conventional and PBG-enhanced spiral inductors, showing good agreements between the theoretical and measured data for the conventional spiral inductor. The series inductance L_s increases by 5%, 6.75%, 9.41%, 17%, 34% at 0.4, 0.8, 1.2, 1.6, 2.0 GHz, respectively. Notice that the spiral inductors become capacitive near 2.4 GHz for both cases.

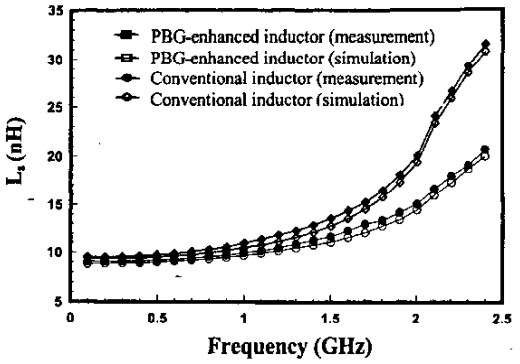

Fig.3 Series inductances of the spiral inductors

The series resistance R_s is one of the dominant factors determining the quality-factor (Q-factor) of the spiral inductor under investigation. The extracted values of R_s from the measured data are plotted in Fig.4 for comparisons. The values of R_s are nearly identical below 1.4 GHz for the PBG-enhanced and conventional spiral inductors. Above 1.4 GHz two curves start to deviate. The value of R_s of the PBG-enhanced spiral inductor is reduced by 39%, 36%, 34%, 45% at 1.6, 1,8, 2.0, 2.2 GHz, respectively. Since the series resistance R_s is related to the compound physical effects of ohmic losses, skin-effect losses and eddy-current losses, and both case studies incorporate the same spiral and the same materials, the results imply that the PBG ground plane reduce the eddy-current losses above 1.4 GHz for our particular case study. The PBG ground plane, however, increases the series inductance at much lower frequency, namely, 6.75% increase of inductance at 0.8 GHz.

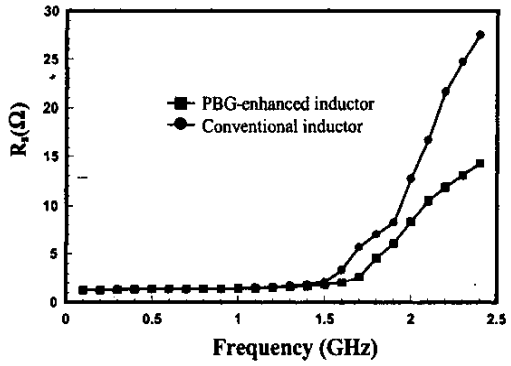

Fig.4 Measured series resistance R_s of PBG-enhanced and conventional spiral inductors

Three main contributing factors to the Q-factor of the spiral inductor are 1) series L_s-R_s, 2) substrate loss factor, and 3) self-resonance factor [6]. Therefore the Q-factor can be expressed by the product of $(\omega L_s/R_s)$, $R_p/(R_p+[(\omega L_s/R_s)^2+1]R_s)$, and $(1-R_s^2(C_p+C_s)/L_s-\omega^2 L_s(C_p+C_s))$.

Fig. 5 compares the quality-factors of the PBG-enhanced and conventional spiral inductors. The conventional spiral inductor has the maximum Q-factor of approximately 50 at 1.4 GHz, whereas the PBG-enhanced inductor is peaked at 1.6 GHz at Q-factor of 72. The Q-factor is improved by approximately 33% for our particular case studies. Since the spiral inductor on PBG ground plane having higher inductance caused by the higher characteristic impedance Z_o of the transmission equivalent circuit, lower eddy-current influences, and the series resistance R_s is decreased by the PBG ground plane, the Q-factor is improved by the proposed structure. It is advantageous to the proposed PBG-enhanced inductor that the peak Q-factor frequency is moved to higher frequency (1.6GHz), approximately 50% increase from the conventional spiral inductor of the case study.

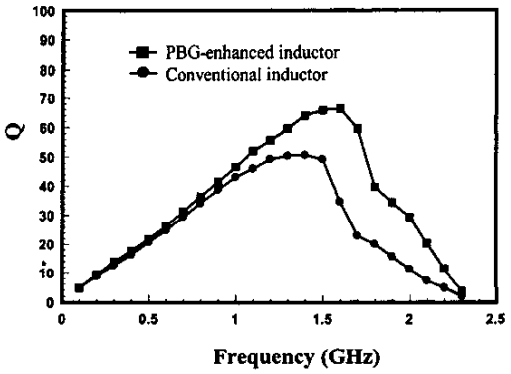

Fig.5 Measured Q-factors of PBG-enhanced and conventional spiral inductors

IV. Conclusion

A novel PBG (photonic bandgap)-enhanced inductor is presented. Measurements of the PBG-enhanced and conventional inductors applying the same spiral show that the PBG ground plane in the new inductor configuration increases the inductance, reduces the series resistance, improves the Q-factor, and extends the peak Q-factor frequency simultaneously.

ACKNOWLEDGEMENT

This work is supported by National Science Council of Taiwan under contract NSC 90-2213-E-009-063 and in connection to project Advanced Technologies for Telecommunications (A) under contract 89-E-FA06-2-4.

REFERENCES

[1] B. Guasticchi, P. Giampolini, L. Roselli, G. Stopponi, "Accurate analysis of silicon, VLSI-Technology Compatible Spiral Inductors," 2000 *IEEE MTT-S Symp. Dig.*, pp. 1157-1160, Jun. 2000.

[2] Nasser Masoumi, Safieddin Safavi-Naeini, Mohamed I. Elmasry, "An efficient and accurate model for RF/Microwave spiral inductors using microstrip line theory," 2000 *IEEE MTT-S Symp. Dig.*, pp. 127-132, Jun. 2000.

[3] David M. Krafcsik, Dale E. Dawson, "A close-form expression for representing the distributed nature of the spiral inductor ," 1986 *Microwave and Millimeter- wave Monolithic Circuits Symp. Dig.* 86-1, pp. 87-92, 1986.

[4] Snezana Jenei, Bart Nauwelaers, Stefaan Decoutere, Abdalla Nacm, "Close form inductance calculation for integrated spiral inductor compact modeling," 2000 *IEEE MTT-S Symp. Dig.*, pp. 131-135, Jun. 2000.

[5] Kenji KAMOGAWA, Kenjiro NISHIKAWA, Tsuneo TOKUMITSU, Masayoshi TANAKA, "A novel high Q inductor based on Si 3D MMIC technology and its application," 1999 *IEEE MTT-S Symp. Dig.*, pp. 489-492, Jun. 1999.

[6] C. Patrick. Yue, Changsup Ryu, Jack Lau, Thomas H. Lee, S. Simon Wong,"A physical model for planar spiral inductors on silicon," 1996 *International Electric Device Meeting*, pp. 155-158, 1996.

[7] Fei-Ran Yang, Yongxi Qian, R. Coccioli, T. Itoh," A novel low-loss slow-wave microstrip structure," *IEEE Microwave Guided Wave Letters*, Vol. 8, No. 11, pp. 372-374, Nov. 1998.

[8] Ching-Kuo Wu, Ching-Kuang C. Tzuang,"Slow-wave propagation of microstrip consisting of electric-magnetic-electric (EME) composite metal strips," 2001 *IEEE MTT-S Symp. Dig.*, pp. 727-730, Jun. 2001.

[9] Ching-Kuo Wu, Hsien-Shun Wu, Ching-Kuang C. Tzuang," Electric-Magnetic-Electric (EME) slow-wave microstrip line and bandpass filter of compressed size," to appear on the August issue of *IEEE Trans. Microwave Theory and Tech.* 2002.